J|A|C|S
ARTICLES
Published on Web 08/09/2002

Nanotubes from the Self-Assembly of Asymmetric Crystalline−Coil Poly(ferrocenylsilane−siloxane) Block Copolymers

Jose Raez, Ian Manners,* and Mitchell A. Winnik*
Contribution from the Department of Chemistry, University of Toronto, 80 St. George Street, Toronto, Ontario M5S 3H6, Canada

Received March 7, 2002

Abstract: Block copolymers with a high asymmetry normally give spherical starlike micelles in a solvent selective for the longer block. We have discovered that samples of poly(ferrocenyldimethylsilane-*b*-dimethylsiloxane) (PFS-*b*-PDMS) with block ratios of 1:12 form nanotubes in *n*-hexane and *n*-decane, which are poor solvents for PFS. Two block copolymer samples PFS_{40}-*b*-$PDMS_{480}$ (M_n = 45 300, PDI = 1.01) and PFS_{80}-*b*-$PDMS_{960}$ (M_n = 90 500, PDI = 1.01) were synthesized by sequential anionic polymerization. When self-assembly occurs, the PFS blocks aggregate and crystallize to form a shell with a cavity in the middle of the tube, while the PDMS blocks form the corona. The nature of these structures was elucidated by conventional transmission electron microscopy and dark-field scanning transmission electron microscopy. Time- and temperature-dependence studies revealed that a variety of morphologies are formed initially depending on the conditions of sample preparation, but most of them eventually rearrange to form nanotubules. The lengths of the tubes can be varied with time and with the choice of solvents. We have been able to grow nanotubes with lengths reaching 0.1 mm. The presence of the hollow core was confirmed by trapping tetrabutyllead in the cavity and performing energy-dispersive X-ray measurements on the resulting structure.

Introduction

Block copolymers self-assemble in selective solvents.[1] For polymers that have a narrow distribution of chain lengths and a common composition, the structures that form are normally uniform in size and have nanometer dimensions. Most diblock copolymers associate to form spherical micelles. A common feature of these structures is that the insoluble block is an amorphous polymer. Under these circumstances, the polymer is referred to as a "coil−coil" diblock copolymer.[2] We have our best theoretical understanding of these structures in two limiting cases. In starlike micelles, the soluble block is much longer than the core-forming block. Repulsive interactions between solvent-swollen coils within the corona lead to chain stretching. The equilibrium size of the micelle is determined by a balance between elastic stretching within the corona, which promotes high curvature and small core size, and the interfacial tension, which promotes an increase in core size to minimize the interfacial area in the system. At the other extreme are crew-cut micelles in which the soluble block is much shorter than the insoluble block. Here the corona consists of short stubby coils of the soluble block. The factor that limits the growth in core size is the stretching of the insoluble polymer, which is necessary to densely fill the core.

Other morphologies are known, particularly for polymers having insoluble amorphous blocks much longer than the soluble blocks. Cylindrical structures have been reported, as well as tubes, vesicles, raftlike layer structures, and compound micelles, whose structure resembles an aggregate of smaller self-assembled structures.[3] Many of these structures are formed under kinetic conditions and then become trapped, for example, by the glassy nature of the insoluble core. It is often difficult to establish that a certain structure represents the equilibrium morphology of a block copolymer-selective solvent system. Within a family of related block copolymers, the morphology one obtains is governed by a number of factors. These include chain length, ratio of the block lengths, polydispersity, chain architecture, solvent composition, temperature, time, concentration, and the details of sample preparation. By manipulating these variables, one can hope to optimize the structures obtained to meet the needs of various applications. Zhang and Eisenberg, for example, demonstrated for polymers that form crew-cut

* To whom correspondence should be addressed. E-mail: mwinnik@chem.utoronto.ca or imanners@chem.utoronto.ca.

(1) Alexandridis, P.; Lindman, B. *Amphiphilic Block Copolymers*; Elsevier Science B. V.: Amsterdam, 2000.
(2) (a) Tuzar, Z.; Kratochvil, P. *Adv. Colloid Interface Sci.* **1976**, *6*, 201. (b) Price, C. *Pure Appl. Chem.* **1983**, *55*, 1563. (c) Xu, R.; Winnik, M. A.; Hallett, F. R.; Riess, G.; Croucher, M. D. *Macromolecules* **1991**, *24*, 87. (d) Zhu, J.; Eisenberg, A.; Lennox, R. B. *J. Am. Chem. Soc.* **1991**, *113*, 5583. (e) Price, C.; Wood, D. *Eur. Polym. J.* **1979**, *9*, 827. (f) Plestil, J.; Baldrina, J. *Makromol. Chem.* **1975**, *176*, 1009. (g) Katoka, T.; Tanaka, T.; Inagoki, H. *Macromolecules* **1978**, *11*, 138. (h) Stacy, C. J.; Krans, G. *Polym. Eng. Sci.*, **1977**, *17*, 627.
(3) (a) Zhang, L.; Eisenberg, A. *J. Am. Chem. Soc.* **1996**, *118*, 3168. (b) Discher, B. M.; Hammer, D. A.; Bates, F. S.; Discher, D. E. *Curr. Opin. Colloid Interface Sci.* **2000**, *5*, 125. (c) Yu, K.; Bartels, C.; Eisenberg, A. *Langmuir* **1999**, *15*, 7157. (d) Ding, J.; Liu, G. *Chem. Mater.* **1998**, *10*, 537. (e) Yu, K.; Eisenberg, A. *Macromolecules* **1998**, *31*, 3509. (f) Won, Y. Y.; Davis, H. D.; Bates, F. S. *Science* **1999**, *283*, 960. (g) Stewart, S.; Liu, G.; *Angew. Chem., Int. Ed.* **2000**, *39*, 340. (h) Shen, H.; Eisenberg, A. *J. Phys. Chem.* **1999**, *103*, 9473. (i) Zhang, L.; Bartels, C.; Yu, Y.; Shen, H.; Eisenberg, A. *Phys. Rev. Lett.* **1997**, *79*, 5034. (j) Ma, Q.; Remsen, E. E.; Clark, C. G.; Kowalewski, T.; Wooley, K. L. *Proc. Natl. Acad. Sci. U.S.A.* **2002**, *99*, 5058.

micelles in water, that they could obtain a variety of different morphologies with a single polymer sample by changing the solvent and salt composition.[4] Those findings provide a glimpse of the complex interplay of factors that affect block copolymer self-assembly.

Another class of diblock copolymers is referred to as rod−coil systems. These polymers consist of a flexible soluble block attached to a rigid, or semirigid second block, which can either be a helical polymer or a stiff conjugated polymer.[5] We have a much poorer theoretical understanding of the structures formed by rod−coil systems[6] than those formed by coil−coil block copolymers.[7]

We are interested in self-assembled structures formed from poly(ferrocenylsilane) (PFS) block copolymers in solution. We have studied a series of these polymers.[8,9] Those in which the insoluble PFS block is amorphous appear to form normal starlike micelles. Some of these polymers form long, thin, relatively flexible cylindrical (wormlike) micelles in simple hydrocarbons solvents in which the PFS block is insoluble. We have attributed the formation of these wormlike structures[8] to the crystallinity of the PFS block.[10] Thus, these polymers fall within the general class of crystalline−coil block copolymers.

When the insoluble block of a block copolymer is able to crystallize, crystal packing forces play a dominant role in determining the structure of the core of the self-assembled objects that form. In the Vilgis and Halperin [11] model, this block forms crystals through adjacent folds within the core, and a sharp interface divides the crystalline core from the solvent-swollen corona. The overall shape of the self-assembled structure depends on the interplay between the interfacial energy between the core and the solvent and stretching within the corona due to overlap of adjacent coils. The corona chains are treated as though they are grafted to the core at a spacing that depends on the number of folds per core block. Thus, the response to strong corona chain repulsion is a larger number of thinner folds in the crystalline core-forming chain. Vilgis and Halperin identified two separate contributions to the interfacial free energy, one due to the interfacial tension σ_f in the fold plane and the other due to the lateral interfacial tension σ_l at the edge of each crystal.

The most common morphology expected from this model is that of flat monolayer or bilayer plates, with the corona chains protruding from both faces.[12] In lamellar structures, a system can minimize the repulsion between adjacent coils of the corona block by increasing the number of folds in the crystalline core, leading to a thinner core, or it can minimize the surface free energy by increasing the fold length, decreasing the spacing between coils of this polymer. The equilibrium structure represents a balance between these two energies. If the soluble block is very long, one can imagine cylindrical or even starlike micelles. Vilgis and Halperin contended that because the core is formed by adjacent folds of a crystalline polymer, the core of a cylindrical micelle does not have a circular cross section but must be formed by the end-to-end packing of a rectangular unit cell.[11] Furthermore, they postulated that starlike micelles formed from polymers with long corona chains have a core in the form of a rectangular solid.

In this paper, we describe the results we obtained with two samples of poly(ferrocenyldimethylsilane)-*block*-poly(dimethylsiloxane) (PFS_{40}-*b*-$PDMS_{480}$ and PFS_{80}-*b*-$PDMS_{960}$) in which the PDMS block is a factor of 12 longer than the PFS block. Unlike the case of PFS_{50}-*b*-$PDMS_{300}$ examined by Massey et al., which formed wormlike micelles in hexane solutions, the 1:12 polymers generate a tubular morphology.[13] We examine the influence of temperature on the structures formed in *n*-hexane and in *n*-decane, and we describe our experiments that were designed to investigate whether the structures that appear to be nanotubes in the electron microscopy images are in fact hollow structures.

Aside from the interesting structures that they form, these block polymers are of interest because the PFS component is a redox-active material with semiconducting properties, and it can also serve as ceramic precursor.[14] Thus, the self-assembled structures may be thought of as precursors to ceramic nanodomains.[15]

Experimental Section

Materials, Synthesis, and Characterization. The solvents *n*-hexane, *n*-nonane, and *n*-dodecane were obtained form Aldrich Co. (99+% pure). *n*-Heptane (99% pure) and *n*-octane (97%) were obtained from Caledon Laboratories Ltd. *n*-Decane was acquired from Fisher Chemicals (99% pure). All of these solvents were used without further purification. Tetrahydrofuran was distilled from Na/benzophenone under prepurified N_2 immediately prior to use. Chlorotrimethylsilane, hexamethyltrisiloxane, and *n*-butyllithium were purchased from Aldrich Co. Chlorotrimethylsilane was distilled before use. Hexamethyltrisiloxane was stirred over CaH_2 in *n*-pentane at room temperature overnight and then distilled under vacuum twice before use. *n*-Butyllithium was used without further purification.

Polymer synthesis was carried out in a Braun model MB20G glovebox at 25 °C in an atmosphere of prepurified nitrogen. Molecular weights were determined by gel permeation chromatography (GPC) with a Waters Associates liquid chromatograph equipped with a Waters 410 differential refractometer and a Viscotek T60A dual detector consisting of a 90° angle laser light scattering detector (λ_o = 670 nm)

(4) Zhang, L.; Eisenberg, A. *Macromolecules* **1996**, *29*, 8805−8815.
(5) (a) Cornelissen, J. J. L. M.; Fischer, M.; Sommerdijk, N. A. J. M.; Nolte, R. J. M. *Science* **1998**, *280*, 1427. (b) Jenekhe, S. A.; Chen, X. L. *J. Phys. Chem. B* **2000**, *104*, 6332. (c) Chen, X. L.; Jenekhe, S. A. *Langmuir* **1999**, *15*, 8007. (d) Kukula, H.; Ziener, U.; Schöps, M.; Godt, A. *Macromolecules* **1998**, *31*, 5160. (e) Leclère, P.; Calderone, A.; Marsitzky, D.; Francke, V.; Geerts, Y.; Müllen, K.; Brédas, J. L.; Lazzoroni, R. *Adv. Mater.* **2000**, *12*, 1042. (f) Lee, M.; Lee, D.-W.; Cho, B.-K.; Yoon, J.-Y.; Zin, W.-C. *J. Am. Chem. Soc.* **1998**, *120*, 13258. (g) Wu, J.; Pearce, E. M.; Kwei, T. K.; Lefebvre, A. A.; Balsara, N. P. *Macromolecules* **2002**, *35*, 1791. (h) Kimura, S.; Kim, D.-H.; Sugiyama, J.; Imanishi, Y. *Langmuir* **1999**, *15*, 4461.
(6) (a) Müller, M.; Schick, M. *Macromolecules* **1996**, *29*, 8900. (b) Halperin, A. *Macromolecules* **1990**, *23*, 2724.
(7) (a) Halperin, A. *Macromolecules* **1987**, *20*, 2943. (b) Halperin, A. *Macromolecules* **1989**, *22*, 2403. (c) Noolandi, J.; Hong, K. M. *Macromolecules*, **1983**, *16*, 1443.
(8) Massey, J.; Temple, K.; Cao, L.; Rharbi, Y.; Raez, J.; Winnik, M. A.; Manners, I. *J. Am. Chem. Soc.* **2000**, *122*, 11577.
(9) (a) Temple, K.; Massey, J. A.; Chen, Z.; Vaidya, N.; Berenbaum, A.; Foster, M. D.; Manners, I. *J. Inorg. Organomet. Polym.* **1999**, *9*, 189. (b) Raez, J.; Manners, I.; Winnik, M. A. *Langmuir* **2002**, in press.
(10) (a) Papkov, V. S.; Gerasimov, M. V.; Dubovik, I. I.; Sharma, S.; Dementiev, V. V.; Pannell, K. H. *Macromolecules* **2000**, *33*, 7107. (b) Chen, Z.; Foster, M. D.; Zhou, W.; Fong, H.; Reneker, D. H.; Resendes, R.; Manners, I. *Macromolecules* **2001**, *34*, 6156.
(11) Vilgis, T.; Halperin, A. *Macromolecules* **1991**, *24*, 2090.
(12) (a) Lotz, B.; Kovacs, A. J. *Kolloid-Z. Z. Polym.* **1966**, *209*, 97. (b) Kawai, T.; Shiozaki, S.; Sonoda, S.; Nakagawa, H.; Matsumoto, T.; Maeda, H. *Makromol. Chem.* **1969**, *128*, 252. (c) Dröscher, M.; Smith, T. L. *Macromolecules* **1982**, *15*, 442. (d) Richter, D.; Schneiders, D.; Monkenbusch, M.; Willner, L.; Fetters, L. J.; Huang, J. S.; Lin, M.; Mortensen, K.; Fargo, B. *Macromolecules* **1997**, *30*, 1053. (e) Lin, E.; Gast, A. *Macromolecules* **1996**, *29*, 4432.
(13) Communication: Raez, J.; Barjovanu, R.; Massey, J. A.; Winnik, M. A.; Manners, I. *Angew. Chem., Int. Ed.* **2000**, *39*, 3862.
(14) MacLachlan, M. J.; Ginzburg, M.; Coombs, N.; Coyle, T. W.; Raju, N. P.; Greedan, J. E.; Ozin, G. A.; Manners, I. *Science* **2000**, *287*, 1460.
(15) (a) Massey, J. A.; Winnik, M. A.; Manners, I.; Chan, V. Z.-H.; Ostermann, J. M.; Enchelmaier, R.; Spatz, J. P.; Möller, M. *J. Am. Chem. Soc.* **2001**, *123*, 3147. (b) Chan, V. Z.-H.; Hoffman, J.; Lee, V. Y.; Iatrou, H.; Avgeropoulos, A.; Hadjichristidis, N.; Miller, R. D.; Thomas, E. L. *Science* **1999**, *286*, 1716.

and a four-capillary differential viscometer. The triple-detector system has been shown to provide absolute M_w values of PFS homopolymers,[16] and we assume that it provides accurate values of M_w/M_n. ^{1}H NMR spectra were taken with a Varian Mercury 300 instrument operating at 300 MHz.

Synthesis and Characterization of Diblock Copolymers. A detailed description of the synthesis of a poly(ferrocenylsilane-*b*-dimethylsiloxane) is presented elsewhere.[17] The first step involves the initiation of the strained silicon-bridged [1]ferrocenophane with *n*-butyllithium and the subsequent addition of hexamethyltrisiloxane (D_3). The reaction was terminated with chlorotrimethylsilane. Before adding D_3 to the reaction, an aliquot of the PFS homopolymer was withdrawn from the reactor and analyzed by GPC. This sample allowed us to determine the weight of the PFS block. The M_n of the homopolymer and the unpurified diblock copolymer were determined by GPC analysis. The block copolymer was then passed through a preparative size exclusion column in THF to eliminate any homopolymer present in the sample. From the composition of the purified diblock copolymer determined from its ^{1}H NMR spectrum in combination with the known M_n of the PFS block, we calculated the degree of polymerization of the block copolymers to be PFS_{40}-*b*-$PDMS_{480}$ and PFS_{80}-*b*-$PDMS_{960}$. ^{1}H NMR (300 MHz, C_6D_6, δ): 0.28 (s,$OSiMe_2$), 0.54 (s, $fcSiMe_2$), 4.10 (s, C_5H_4), 4.27(s, s, C_5H_4). Block ratio of PFS:PDMS = 1:12.

Preparation of Micelle Solutions. All micelle solutions described in this paper have a concentration of 1.0 g/L. To ensure reproducibility, all experiments were repeated at least three times. Experiments in *n*-hexane and *n*-decane examine the temperature- and time-dependent changes in micelle morphology.

(a) Experiments in *n*-Hexane. When a sample of solid PFS-*b*-PDMS is dispersed by agitation in *n*-hexane at room temperature (23 ± 0.5 °C), a clear solution forms. Samples were collected over time (immediately/within 5 min, 1 day, 3 days, 1 week, 3 weeks, and 3 months) for transmission electron microscopy (TEM) analysis. Samples were also prepared by adding *n*-hexane (10 mL, bp 68 °C) to the diblock copolymer (10 mg) in a flask or vial, which was then placed in a preheated oil bath at 61 ± 0.5 °C for 30 min to 1 h. TEM samples were prepared at this temperature by quickly spraying the micellar solution onto a carbon film or by immersing a precoated copper grid into the solution. Then the mixture was cooled to room temperature over a period of 2 h. Samples were then collected over time.

(b) Experiments in *n*-Decane. Micelle solutions in *n*-decane (bp 174 °C) were prepared by adding 10 mL of solvent to 10 mg of block copolymer in a vial or flask, which was then placed in a preheated oven or oil bath at 151 ± 0.5 °C for 30 min to 1 h. *n*-Decane does not dissolve the block copolymer at room temperature. An aliquot was withdrawn and immediately quenched in an ice bath. TEM samples were then prepared by placing a 7-μL sample on a precoated copper grid. Excess fluid was then removed with a clean piece of filter paper. Samples were also prepared by quickly spraying a 20-μL sample of the micellar solution at 151 °C onto a carbon film. The rest of the micellar solution was allowed to cool to room temperature over a period of 6 h. Samples were then collected over time.

To explore the effects of temperature on sample preparation, the block copolymer was also heated in *n*-decane in a preheated oil bath at 61 °C for 30 min to 1 h. TEM samples were prepared at this temperature by placing a 7-μL sample of the micellar solution onto a precoated copper grid, which was placed on a filter paper, or by immersing a precoated copper grid into the solution. Excess fluid was then removed with a clean piece of filter paper. The mixture was allowed to cool to room temperature over a period of 2 h. Samples were then collected over time.

Scheme 1

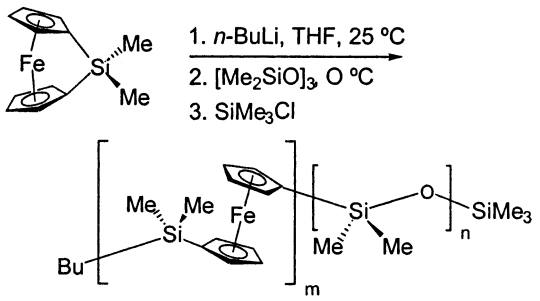

(c) Encapsulation of Tetrabutyllead. A sample of the block copolymer PFS_{40}-*b*-$PDMS_{480}$ (10 mg) was dissolved in *n*-hexane (10 mL) at room temperature. Once the solution became homogeneous, tetrabutyllead (100 mg, Gelest Inc.) was added, and the solution was stirred at room temperature for 2 days. An aliquot of the solution was removed, and a sample for TEM analysis was prepared by spraying 20-μL of this solution onto a carbon film onto a mica substrate.

Transmission Electron Microscopy and Energy-Dispersive X-ray Measurements. Samples for TEM were prepared by aerosol spraying a micellar solution (20 μL) onto a carbon film (~50 Å) grown on mica, then floated off the mica, and placed on a 300-mesh gilder copper TEM grid. To explore the effects of sample preparation on the micellar morphology, TEM samples were also prepared by placing a 7-μL aliquot onto a precoated copper grid and removing the excess fluid with a clean piece of filter paper. Precoated copper grids were prepared by floating a clean carbon film onto water and depositing the film on the copper grids. No staining was necessary to image the PFS blocks by TEM.

To visualize the entire micelle structure, our samples were coated with Pt/C. For Pt/C shadow casting, the micelle sample on carbon-coated mica was placed in a high-vacuum chamber coater (Edwards, model E12E4) above a 5-mm spherical platinum source on a carbon substrate. Pt/C atoms were vaporized onto the mica at a 30° angle at high voltage at 10^{-5} Torr. The sample was then floated onto several 300-mesh copper grids.

TEM images were obtained with a Hitachi model 600 electron microscope at 75 kV. Before every TEM session, the electron beam was aligned to minimize optical artifacts. Energy-dispersive X-ray (EDX) analysis was performed using a JEM2010F HRTEM/STEM field emission electron microscope at 200 kV, using a Link Pentafet-Oxford detector connected to an ISIS software (McMaster University, Hamilton, ON, Canada).

Wide-Angle X-ray Scattering. Samples for wide-angle X-ray-scattering (WAXS) measurements were prepared by casting a film from a micelle solution (1 mg/mL) in *n*-hexane at room temperature onto an aluminum substrate, followed by spontaneous evaporation of the solvent. The films were ~10 μm thick. WAXS diffraction data were obtained with a Siemens D500 $\theta/2\theta$ diffractometer with a Cu Kα source operating at 50 kV and 35 mA in the step scan mode.

Contact Angle Measurements. Contact angles were measured with a Brice-Phoenix differential refractometer at 23 °C. A film of poly(ferrocenyldimethylsilane) was prepared by solvent casting from toluene and left under vacuum for 2 days. To measure the angles, the flat film was placed on a glass slide. Angles were measured as soon as a 3-μL drop of solvent (*n*-heptane, *n*-octane, *n*-nonane, *n*-decane, and *n*-dodecane) was placed on the film. After 3 min, the contact angles were measured again. In the case of *n*-heptane and *n*-octane, the drops evaporated after 3 min. All angles reported are averaged from repeated measurements.

3. Results

Samples of well-defined PFS-*b*-PDMS were synthesized by living anionic ring-opening polymerization as shown in Scheme

(16) Massey, J. A.; Kulbaba, K.; Winnik, M. A.; Manners, I. *J. Polym. Sci. Polym. Phys.* **2000**, *38*, 3032.
(17) Massey, J.; Power, K. N.; Manners, I.; Winnik, M. A. *J. Am. Chem. Soc.* **1998**, *120*, 9533.

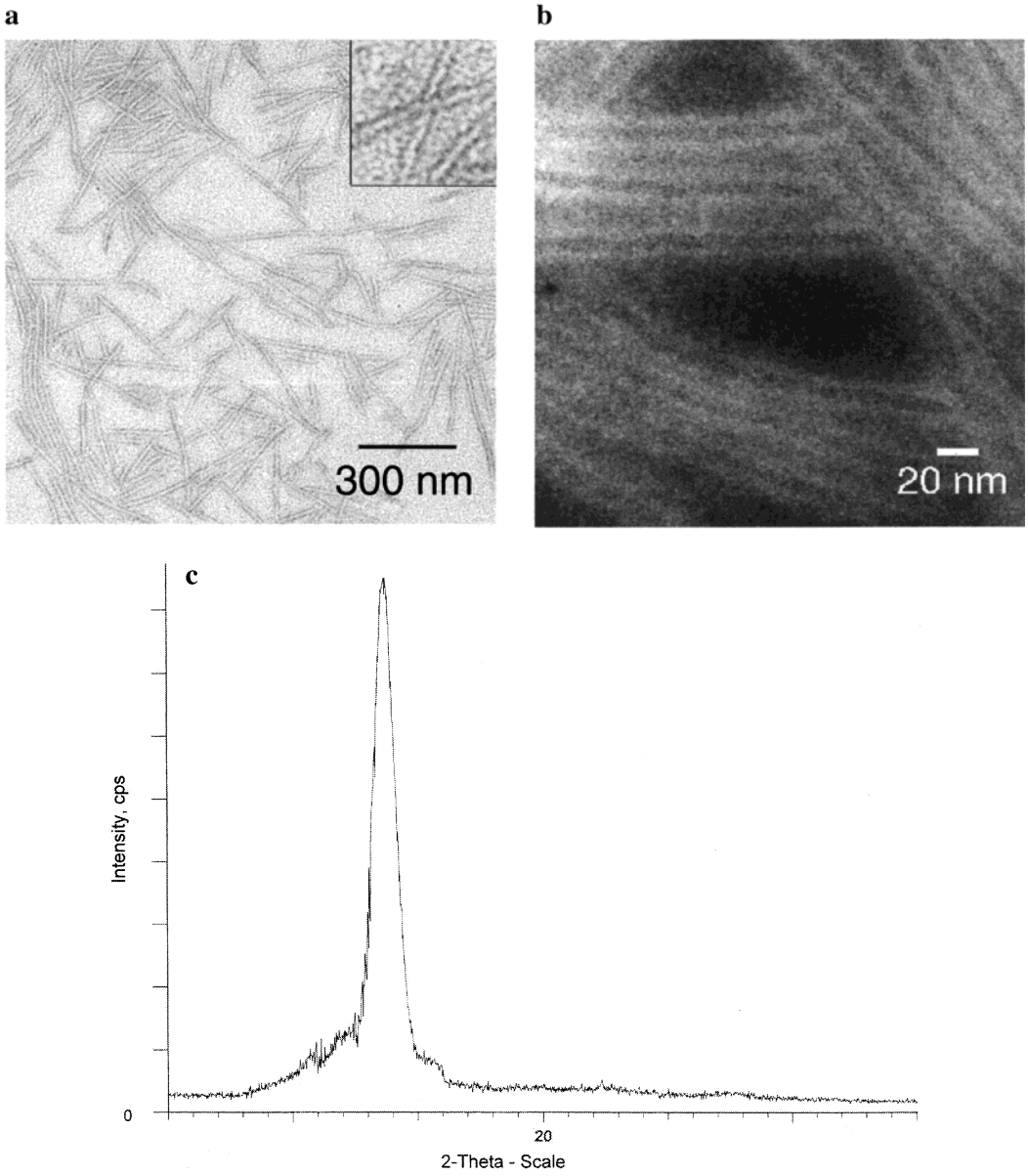

Figure 1. TEM micrograph of PFS_{40}-*b*-$PDMS_{480}$ assemblies formed in *n*-hexane at room temperature. The samples were aerosol-sprayed onto a carbon film. Samples were viewed (a) under bright-field mode in a CTEM (b) and under dark-field mode in a STEM. The inset in (a) shows a section of the image at enhanced magnification. In this and subsequent figures, the insets correspond to an area of 150 nm × 150 nm. (c) WAXS pattern of film of PFS_{40}-*b*-$PDMS_{480}$ assemblies prepared in *n*-hexane at room temperature.

Table 1. Characterization of the PFS-*b*-PDMS Samples

	polymer	M_n (PFS)[a]	M_n (diblock)[a]	block ratio[b]	M_n (diblock)[c]	PDI[a]
1	PFS_{40}-*b*-$PDMS_{480}$	9 700	46 800	1:12	45 300	1.01
2	PFS_{80}-*b*-$PDMS_{960}$	19 300	105 200	1:12	90 500	1.01

[a] Determined by GPC analysis. [b] Determined by ^{1}H NMR analysis. [c] Determined from M_n(PFS) and ^{1}H NMR analysis.

1. The first step involves the initiation of the strained silicon-bridged [1]ferrocenophane with *n*-butyllithium and the subsequent addition of hexamethyltrisiloxane (D_3). The reaction was terminated with chlorotrimethylsilane. The crude product was purified by preparative size exclusion chromatography column in THF.

To study the effect of molecular weight on self-assembly at a given block ratio, we prepared two polymers differing by a factor of 2 in molecular weight. The characteristics of these polymers are presented in Table 1.

PFS_{40}-*b*-$PDMS_{480}$. (1) Experiments in *n*-Hexane. We begin by examining the aggregates formed when a sample of solid PFS_{40}-*b*-$PDMS_{480}$ is dispersed by agitation in hexane at room temperature (23 °C). TEM images of these aggregates show that they have a tubular morphology (Figure 1a). These nanotubes have contour lengths ranging from 60 to 600 nm, an average wall thickness of 7 nm, and a cavity width of 9 nm. Although the length of these micelles is polydisperse, the width of these tubes (∼23 nm) and that of the cavity (9 nm) are relatively uniform. From previous experience, we have learned that, in unstained TEM images of PFS-*b*-PDMS cylindrical structures, we are only able to see the electron-rich PFS domains.[8,17] Thus, we infer that the walls of the tubes are formed by the PFS blocks. When the *n*-hexane solutions described above

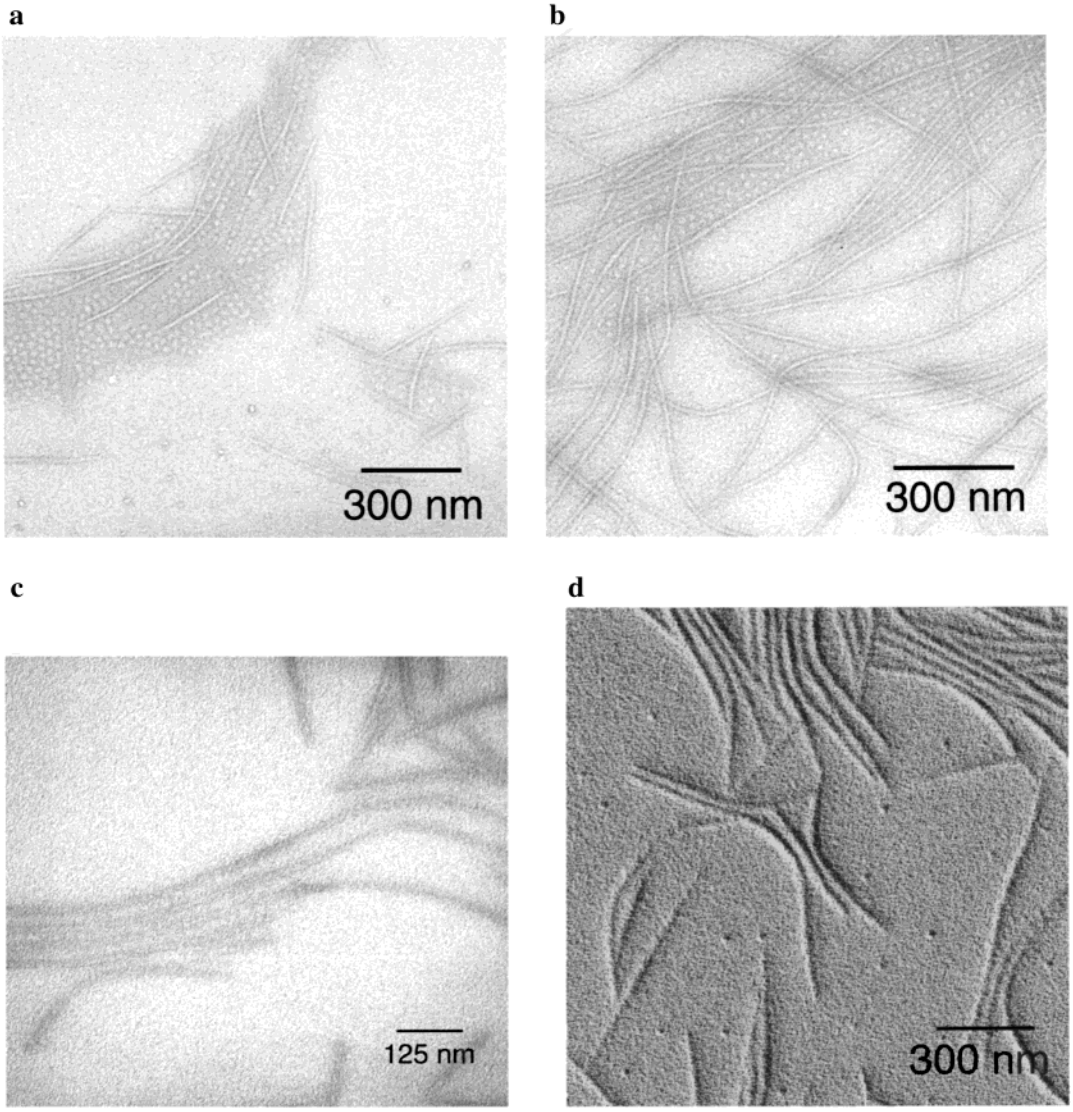

Figure 2. TEM micrographs of PFS_{40}-*b*-$PDMS_{480}$ assemblies prepared in *n*-hexane at 61 °C. In (a) the sample was prepared at 61 °C. In (b) the solution was cooled to room temperature and allowed to age for 3 days. (c) is a higher magnification micrograph of the sample in (b). (d) shows assemblies similar to those in (b) coated with Pt/C at an angle of 30°. Samples for TEM analysis were aerosol-sprayed onto a carbon film.

were allowed to age in the dark at room temperature, no changes were observed by TEM over a 3-month period. We also found identical structures when the samples for TEM were prepared by aerosol spraying or solvent casting from *n*-hexane.

Figure 1b shows a high resolution/scanning TEM (HRTEM/STEM) micrograph in the dark-field mode. In dark field, the cores of the structures, which we assign to the nanotube cavity, appear darker than the shells of the tubes but slightly lighter than the background. This result is consistent with a tubular structure with electron-rich walls. We prepared a sample for WAXS measurements by solvent casting from the micellar solution described above. The solvent was allowed to evaporate at room temperature. The WAXS pattern shows a single strong reflection at 6.48 Å and a halo at the base of the peak from the amorphous regions in the sample (Figure 1c).

Another method by which we prepared polymeric micelles consisted of adding *n*-hexane to a known amount of solid polymer **1** (1.0 g/L), and heating the mixture for 30 min to 1 h at 61 °C (Figure 2). This temperature is above the glass transition temperature of PFS (T_g = 34 °C).[18] Samples for TEM measurements were prepared by quickly spraying small amounts (20 μL) of the hot solution onto a carbon film or by immersing a precoated copper grid in the solution. Figure 2a is a representative TEM image of the sample prepared by spraying. It shows aggregates that appear to be a mixture of nanotubes and hollow spheres. The lengths of these tubes range from 250 to 400 nm, with widths similar to the nanotubes shown in Figure 1a,b. The spherical objects appear to be relatively monodisperse in size with a diameter similar to the width of the tubes (~23 nm). This solution was allowed to cool slowly to room temperature over a period of 2 h. An aliquot was sprayed onto a carbon film and viewed under TEM. No significant changes in the morphology or the distribution of different species were observed when compared to the sample shown in Figure 2a.

This sample was allowed to age for 3 days at room temperature. Samples for TEM were prepared by spraying an aliquot onto a carbon film. The image taken is shown in Figure 2b, where we observe that lengths of the tubes reach 2 μm, while their widths remain constant at ~23 nm. The images taken

(18) Manners, I. *Chem. Commun.* **1999**, 857.

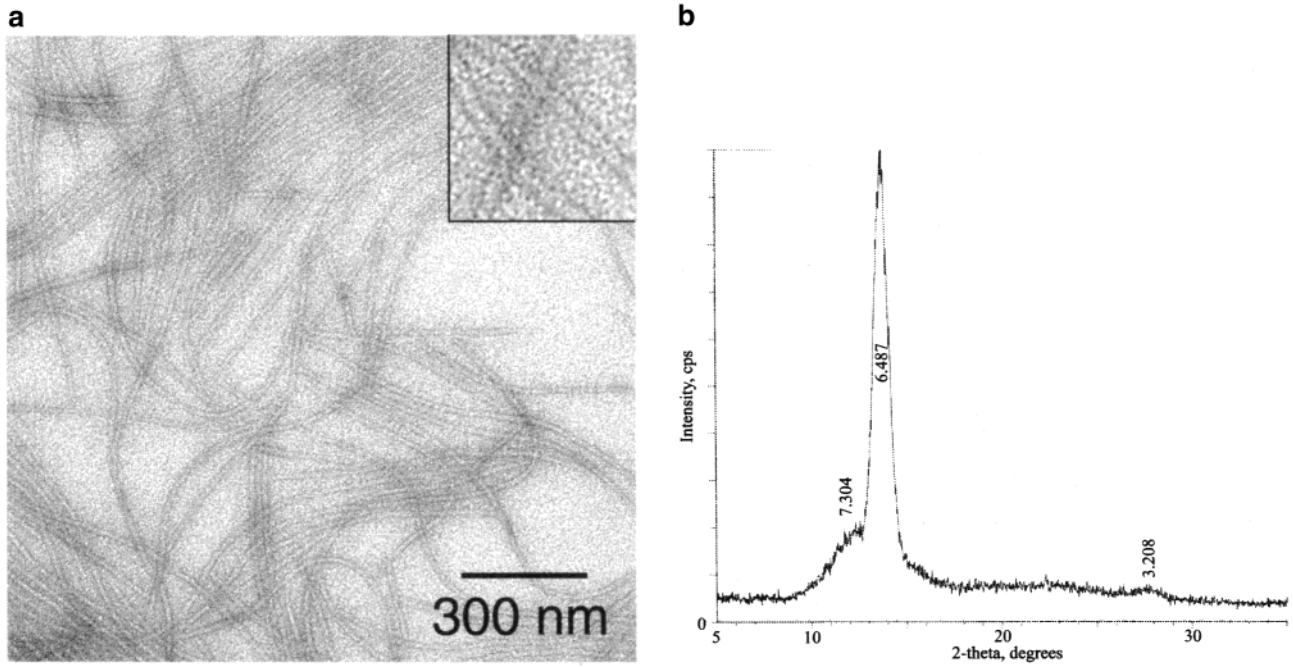

Figure 3. (a) TEM micrograph of PFS_{40}-*b*-$PDMS_{480}$ assemblies prepared in *n*-hexane at 61 °C and cooled to room temperature and left to age for 1 week. The inset shows a section of the image at enhanced magnification. The solution was then allowed to age for 1 week. Samples for TEM analysis were aerosol-sprayed onto a carbon film. (b) WAXS pattern of a film of PFS_{40}-*b*-$PDMS_{480}$ assemblies from (a).

for this aged sample show a significantly smaller population of hollow spheres than in the images of the samples prepared initially at 61 °C (Figure 2a). Figure 2c is a high magnification micrograph of the tubes present in Figure 2b.

Figure 2d is a TEM image showing aggregates from Figure 2b that were shadowed with platinum/carbon (Pt/C) at 30°. Based on the angle of shadowing and the length of the shadow, we calculated the height of the tubes to be 14−17 nm, whereas the overall width ranges from 36 to 40 nm. When the objects are coated with Pt/C, we are no longer able to see the cavity of the tubes or spheres in the sample.

One week after preparing the solution at 61 °C, we prepared a sample for TEM by spraying an aliquot onto a carbon film (Figure 3a). Here we find that the length of the tubes has reached ~4 μm and that the spheres are no longer present. The widths of these tubes are the same as the ones observed in Figure 2b. A film prepared from this solution was analyzed by WAXS. Figure 3b shows the WAXS pattern of the film, which reveals a strong reflection at 6.49 Å, a moderate reflection at 7.30 Å, and a weak peak at 3.21 Å.

(2) Experiments in *n*-Decane. We examined aggregates formed in *n*-decane by adding the solvent to a sample of solid PFS_{40}-*b*-$PDMS_{480}$ in a vial (1.0 g/L) and heating it at 151 °C (above the T_m of PFS, 122−143 °C).[18] Although the diblock copolymer itself is not soluble in *n*-decane at room temperature, heating produces a homogeneous solution, which remains clear upon cooling back to room temperature. After the solution was heated at 151 °C for 30 min, a 20-μL aliquot of the hot solution was rapidly sprayed onto a carbon film. Another 1-mL aliquot was quenched in an ice bath, and a 7-μL drop of the cold solution was placed on a precoated copper grid. Excess fluid was withdrawn with a piece of filter paper. Both samples gave similar TEM images. Thus, we conclude that sample preparation by either method does not affect the morphologies found in the TEM images. Figure 4a is a representative TEM micrograph showing the aggregates formed at 151 °C. These aggregates are dense spherical micelles, with PFS core diameters ranging from 10 to 15 nm.

The micelle solution was then allowed to cool to room temperature over a period of 6 h. Samples were prepared by placing a 7-μL drop on a precoated copper grid. Figure 4b is a TEM image of the sample prepared in this way. One sees aggregates with irregular morphologies and sizes ranging from 750 nm to 3.5 μm in length. After this solution was allowed to age for 5 days at room temperature, another sample for TEM was prepared (Figure 4c). Here we see an example of an unusual morphology in which a single cylindrical object appears to have grown out of a large aggregate.

When this same solution was allowed to age 3 weeks at room temperature, the images seen in the TEM are very different. Now only long nanotubes are observed, with an average shell thickness of 7 nm and a cavity 7 nm wide (Figure 5a). The tubules are so long that a single low-magnification micrograph is not sufficient to measure the contour length (Figure 5b). However, by scanning through large areas in the microscope, we are able to estimate the lengths as up to ~0.1 mm. We did not observe any further changes in the morphology of the aggregates in the solution over a period of 6 months.

We then explored the formation of aggregates in *n*-decane at 61 °C. We prepared the solution by adding *n*-decane to a sample of solid PFS_{40}-*b*-$PDMS_{480}$ in a flask, which was then placed in a preheated oil bath. After maintaining this temperature for 30 min, a 7-μL drop was placed on a precoated copper grid placed on a filter paper. As soon as the drop came into contact with the grid, the excess fluid was immediately absorbed by the filter paper. We hoped that this method would minimize the cooling time of the sample before the solvent was removed. Other samples for TEM were prepared by dipping a precoated copper grid into the micellar solution at 61 °C. TEM images from both types of samples show the presence of a mixture of spherical

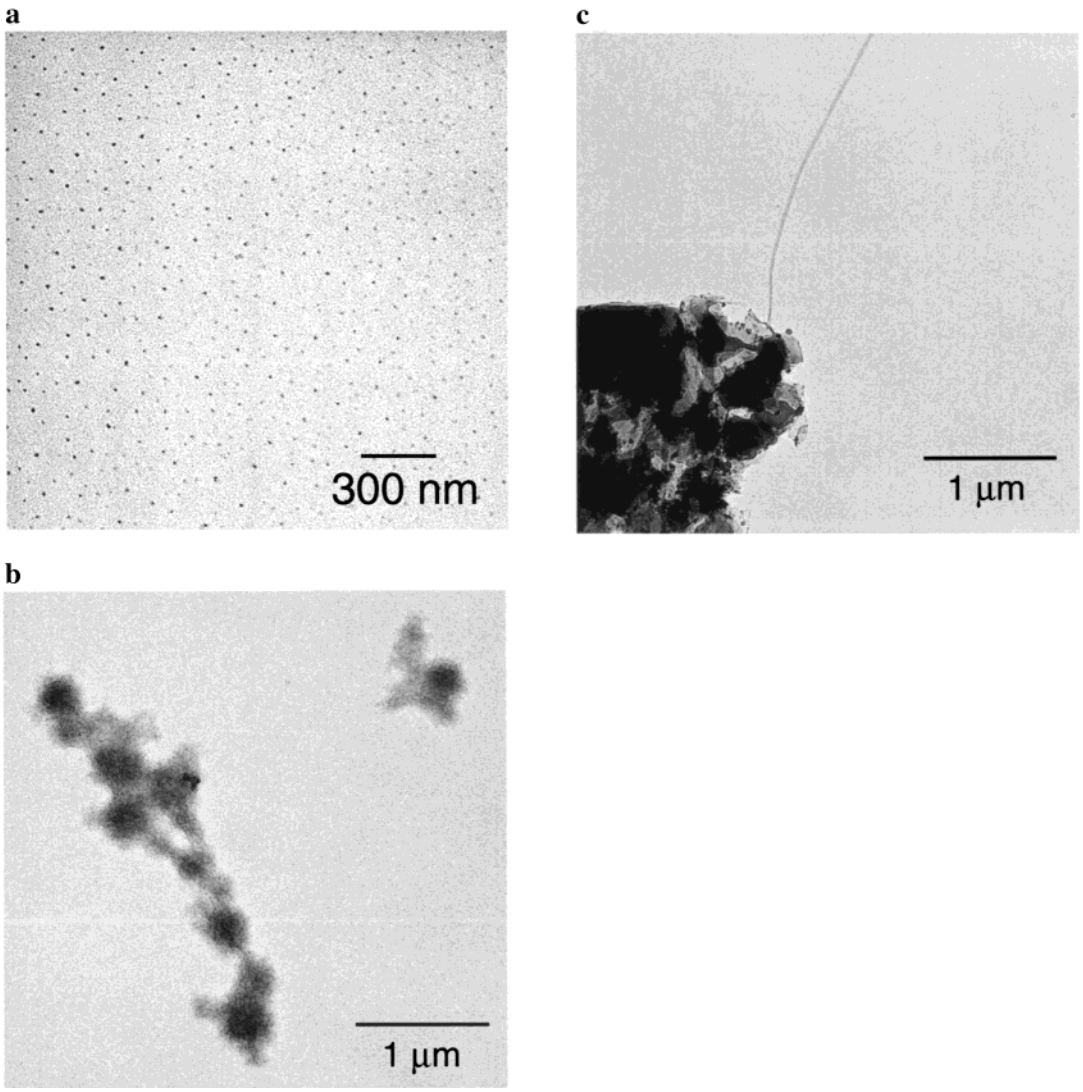

Figure 4. TEM micrographs of PFS_{40}-*b*-$PDMS_{480}$ assemblies formed in *n*-decane prepared at 151 °C. In (a) the sample was aerosol-sprayed at 151 °C onto a carbon film. In (b) the solution was cooled to room temperature over a period of 6 h. In (c) the solution was examined by TEM after 5 days at in *n*-hexane at 23 °C. Samples for TEM analysis in (b) and (c) were prepared by placing a 7-μL drop of the solution onto a precoated copper grid.

micelles with diameters of 10−12 nm and dense wormlike micelles with diameters of ∼15 nm (Figure 6a). The cylindrical micelles have lengths ranging from 60 to 200 nm.

After cooling the solution to room temperature over 2 h, a sample was taken and examined by TEM. We see in Figure 6b that only nanotubes are present. The width of these nanotubes is similar to those prepared in the previous experiment (Figure 5a), and the lengths here reach 3 μm. Nanotubes with lengths reaching 100 μm (as in Figure 5b) can be grown by allowing the solution to stand for 1 day at room temperature.

(3) Encapsulation of Tetrabutyllead. We attempted to encapsulate tetrabutyllead (Pb(*n*-Bu)$_4$) inside nanotubes formed from PFS_{40}-*b*-$PDMS_{480}$. We first prepared the aggregates (1 mg/mL) in *n*-hexane at room temperature (Figure 1a). A small amount of Pb(*n*-Bu)$_4$ (100 mg) was added to 10 mL of the micellar solution, and then the mixture was stirred for 2 days. A 20-μL sample of this mixture was sprayed onto a carbon film, and then the carbon film was floated off onto a series of copper grids. Figure 7a is a TEM micrograph of the sample obtained in this way. The widths of the structures are ∼20 nm, and the cavity is no longer visible. Pb(*n*-Bu)$_4$ is relatively volatile. In designing this experiment, we imagined that any excess Pb(*n*-Bu)$_4$ that was not trapped inside the aggregates would spontaneously evaporate inside the high-vacuum sample chamber of the TEM. We carried out EDX measurements on a single aggregate (Figure 7b). The EDX spectrum contains peaks that can be assigned to the presence of Fe ($M\alpha^1 = 6.40$ keV) from the ferrocene groups in PFS, Si ($K\alpha^1 = 1.74$ keV) from the silane and siloxane groups in PFS and PDMS, respectively, and Pb ($M\alpha^1 = 2.34$ keV, $L\alpha^1 = 10.6$ keV) from the encapsulated lead compound. The peaks for both Pb and Fe are very weak, barely visible above the background noise. Despite repeated experiments in order to improve the quality of the EDX data, we obtained reproducibly similar results.

PFS_{80}-b-$PDMS_{960}$. The methods used to prepare micellar solutions and samples for TEM were the same as those described in the previous section (PFS_{40}-*b*-$PDMS_{480}$).

(1) Experiments in *n*-Hexane. We begin by exploring the types of aggregates formed when a sample of solid PFS_{80}-*b*-$PDMS_{960}$ (polymer **2**) is dispersed at 1 mg/mL in *n*-hexane at room temperature to form a transparent solution. A sample from the solution was sprayed on a carbon film and imaged under

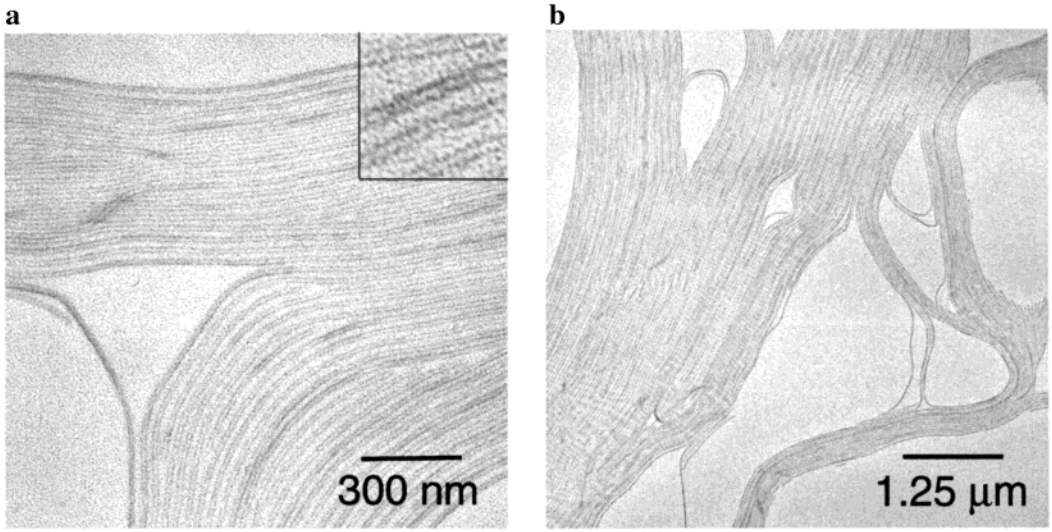

Figure 5. TEM micrographs of PFS_{40}-*b*-$PDMS_{480}$ assemblies prepared in *n*-decane at 151 °C and cooled to room temperature. Samples were imaged (a) after 3 weeks. The inset shows a section of the image at enhanced magnification. (b) is a lower magnification image of the sample in (a). Samples for TEM analysis were prepared by placing a 7-μL drop of the solution onto a precoated copper grid.

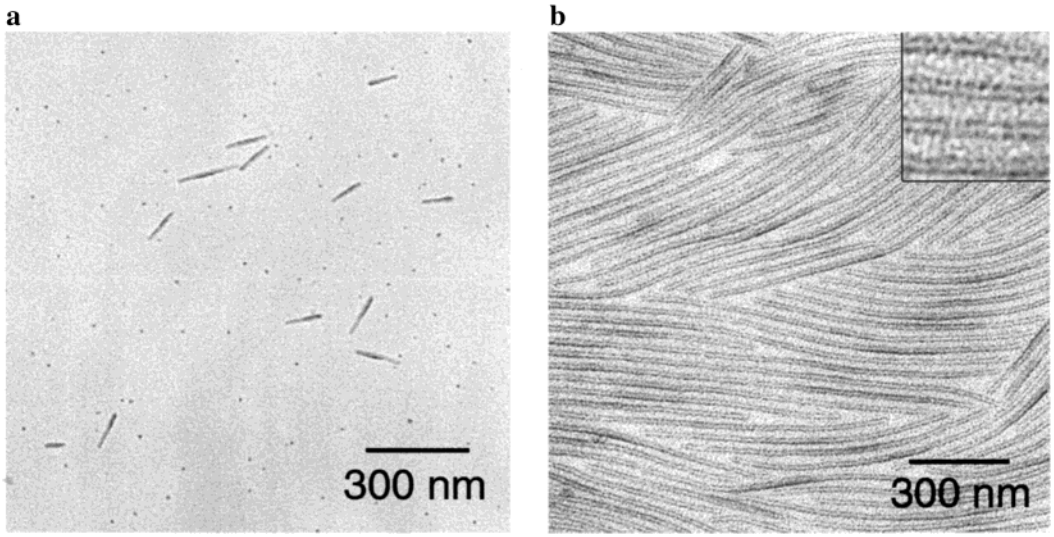

Figure 6. TEM micrographs of PFS_{40}-*b*-$PDMS_{480}$ assemblies formed in *n*-decane at 61 °C. (a) Image of the initially prepared sample. (b) After cooling to 23 °C over a period of 2 h. The inset shows a section of the image at enhanced magnification. Samples for TEM analysis were prepared by placing a 7-μL drop of the solution onto a precoated copper grid at room temperature.

TEM (Figure 8a). The micrograph shows the presence of nanotubes with a PFS wall thickness of 7 nm, a cavity width of 11−12 nm, and lengths reaching 2 μm. In addition, one can see that spherical objects are also present. These have similar overall diameters, but it is very difficult to tell whether they are hollow.

We let the solution age for 1 week at room temperature and then prepared another sample for TEM (Figure 8b). Here we see that only nanotubes are present, and no spherical aggregates can be observed. Wall and cavity thicknesses are similar to those shown in Figure 8a, but the nanotubes themselves are 4 μm long. A 3-day-old sample from the micellar solution described above was sprayed onto a carbon film and shadowed with Pt/C at an angle of 30° (Figure 8c). Based on the angle of shadowing, we calculate the height of both the tubes and spherical aggregates to be 15−18 nm, whereas the overall width ranges from 45 to 52 nm.

We also examined the aggregation of polymer **2** in *n*-hexane by dissolving a solid sample of the polymer at 61 °C. While this temperature was maintained, TEM samples were prepared both by aerosol spraying and by immersing a precoated copper grid in the solution. Figure 9a is a TEM micrograph of the sample prepared by spraying. It shows both hollow spheres and tubular aggregates with lengths reaching 2 μm. The thickness of the PFS shell is 7 nm and the cavity is ∼12 nm wide. The hollow spheres have a shell thickness of 6 nm. The solution was allowed to cool to room temperature over a period of 2 h. An aliquot was then sprayed onto a carbon film and viewed under TEM. The sample showed no significant changes in the morphology or the distribution of species from those observed in Figure 9a. The micellar solution was allowed to age for 2 weeks at room temperature. Samples for TEM were prepared by spraying an aliquot onto a carbon film (Figure 9b). We see in the micrograph that the nanotubes are up to 4 μm in length, and no spherical aggregates are present.

(2) Experiments Performed in *n*-Decane. We examined the aggregation of polymer PFS_{80}-*b*-$PDMS_{960}$ in *n*-decane above the T_m of PFS by adding the solvent to a known amount of

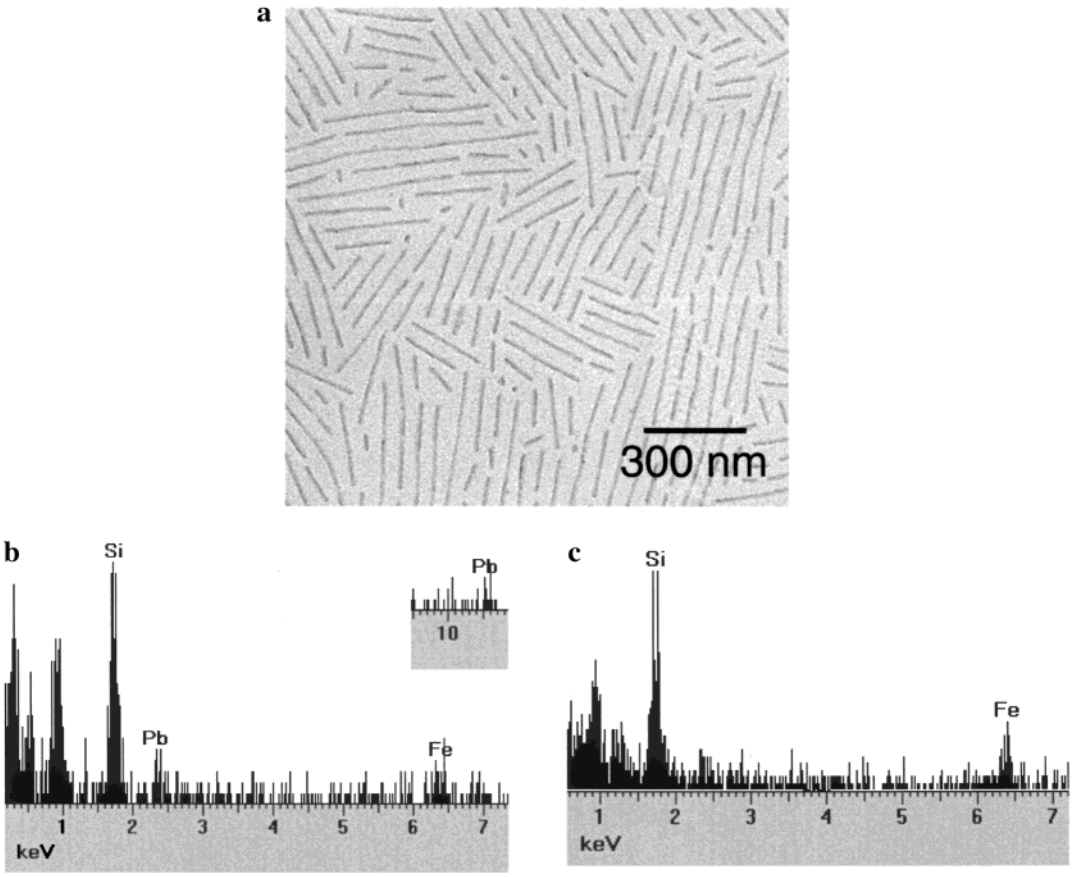

Figure 7. (a) TEM micrograph of PFS_{40}-*b*-$PDMS_{480}$ assemblies formed in *n*-hexane at room temperature after being stirred with Pb(*n*-Bu)$_4$ for 2 days. The sample was aerosol-sprayed onto a carbon film. (b) EDX spectrum of a single assembly shown in (a). (c) EDX spectrum of a single dense wormlike micelle (PFS_{50}-*b*-$PDMS_{265}$) after being stirred with Pb(*n*-Bu)$_4$ in *n*-hexane for 2 days.

solid polymer and then heating the mixture at 151 °C. After 30 min, samples for TEM were prepared. Figure 10a is a TEM image of a sample prepared by spraying 20 μL of the hot solution onto a carbon film. It shows the presence of small dense spherical objects with diameters ranging from 6 to 15 nm. After cooling the micellar solution to room temperature over a period of 6 h, a small portion of the material precipitated out of solution. A 7-μL aliquot of the soluble portion was collected and a sample for TEM was prepared. Figure 10b is an image of this sample, and it shows the presence of small spherical aggregates (~15 nm in diameter) and compound aggregates up to 200 nm in diameter. After this solution aged for 3 months at room temperature, we prepared samples for TEM. These images showed structures essentially the same as those shown in Figure 10b.

We also examined the aggregation of this polymer in *n*-decane at 61 °C. After the mixture was heated for 30 min, a sample for TEM was prepared by placing a 7-μL drop of the hot solution on a precoated copper grid. Figure 11a is a TEM micrograph showing the presence of compound spherical aggregates coexisting with cylindrical structures. The lengths of these cylindrical aggregates range from 250 nm to 2 μm, and the overall diameters vary between 15 and 45 nm. Some of these aggregates appear to be tubular. It is noteworthy that polymer PFS_{80}-*b*-$PDMS_{960}$ did not completely dissolve in *n*-decane at 61 °C; only about half of the material dissolved.

We then let the solution cool to room temperature over a period of 2 h. Another sample for TEM was prepared. In these images, the cylindrical aggregates appear to have grown. The lengths of the cylinders range from 1 μm to tens of micrometers (Figure 11b). The widths of these aggregates are not uniform, and most of them appear to be dense cylinders. In these samples, the population of compound spherical aggregates appears to be smaller than in Figure 11a.

We allowed the solution to age for 1 day at room temperature, and another sample for TEM was prepared. The TEM micrograph of this sample showed well-defined cylindrical aggregates as the only structures in the sample (Figure 11c). Most of them appear to have a tubular morphology, with lengths up to 100 μm. The widths range from 24 to 35 nm. Table 2 summarizes the dimensions of the tubular structures observed in this study. We list the diameters of the cavities, the PFS wall thicknesses, and the contour lengths. The sizes listed in the table are those of the nanotubular morphologies that did not change over a time scale of months.

Discussion

Wide-Angle X-ray Scattering. PFS is a crystalline polymer.[10,18] A detailed crystal structure has been reported for single crystals of the pure pentamer.[19] Many of the reflections characteristic of the pentamer appear in the WAXS pattern of a high molecular weight nonoriented PFS film, which revealed a main reflection at 6.36 Å.[10a] We have expressed the view that the nonspherical morphologies we observe with PFS diblock

(19) Rulkens, R.; Lough, A. J.; Manners, I.; Lovelace, S. R.; Grant. C.; Geiger, W. E. *J. Am. Chem. Soc.* **1996**, *118*, 12683.

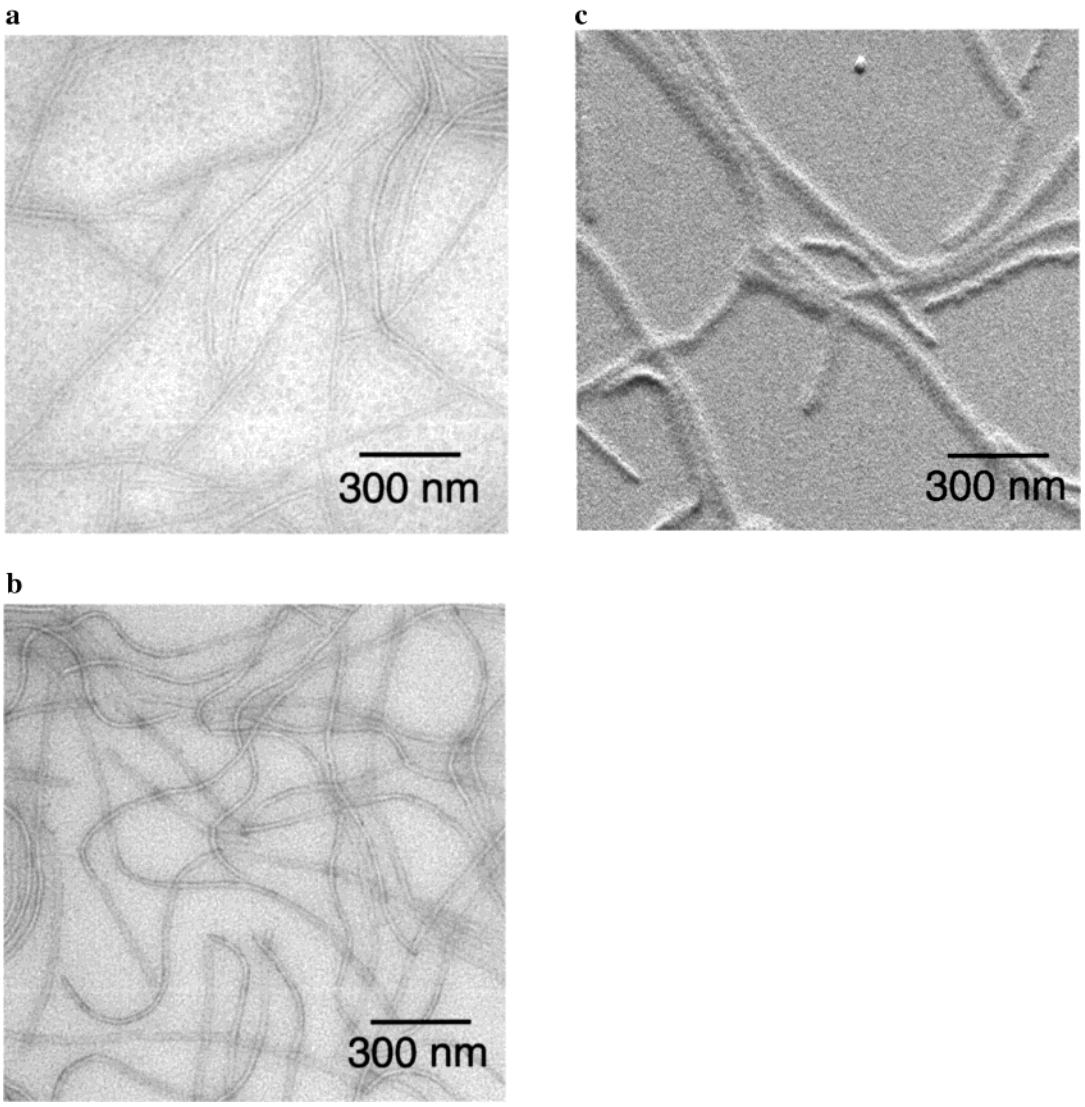

Figure 8. TEM micrographs of PFS_{80}-*b*-$PDMS_{960}$ assemblies prepared in *n*-hexane at room temperature. In (a) the sample was prepared immediately after dissolution. In (b) the sample was prepared after 1 week. In (c) the sample was allowed to age for 3 days and then coated with Pt/C at an angle of 30°. Samples for TEM analysis were aerosol-sprayed onto a carbon film.

copolymers arise as a consequence of the crystallinity of the PFS block.[8] In the examples reported here, the crystallinity of the PFS block is supported by the single reflection at 6.48 Å in the WAXS pattern (Figure 1c). Since PDMS is in its melt state at room temperature, PFS is the only domain able to provide such a reflection. Interestingly, the WAXS pattern of nanotubes formed by initial heating at 61 °C (Figure 3b) shows three reflections, while the WAXS pattern of the nanotubes formed at room temperature shows only one reflection (Figure 1c). We can observe in Figure 3b a very weak peak at 3.21 Å, which is consistent with a second-order reflection (roughly half the value of 6.49 Å). Furthermore, the amorphous region between the diffraction angles 15° and 16° in Figure 1c is no longer present in Figure 3b. This information suggests that PFS chains are slightly more ordered in nanotubes formed at 61 °C than in those formed at room temperature.

Encapsulation, STEM, and Pt/C Shadowing Experiments. In this section, we examine evidence that the tubular structures seen in many of the TEM images are in fact hollow. We also try to infer from the Pt/C shadowing experiments if they are round.

Under conventional transmission electron microscopy (CTEM), the elongated aggregates appear to be hollow. However, optical artifacts, such as Fresnel fringes, associated with defocusing can make a dense cylinder appear as a tube. To test for this possibility, we carried scanning transmission electron microscopy (STEM) measurements in the dark-field mode. In this technique, one monitors electron backscattered from the specimen by a detector, and optical aberrations can be minimized.[20] The STEM micrograph shown in Figure 1b shows that the same aggregates seen in Figure 1a also appear hollow in the dark-field image. The STEM image shows the presence of structures consistent with nanotubes having electron-rich shells formed from the crystalline PFS blocks.

Further evidence to support the presence of a cavity comes from encapsulation experiments with $Pb(n\text{-}Bu)_4$. We chose this lead derivative for three reasons. First, we wanted to use a *n*-hexane-soluble compound containing an electron-rich atom

(20) (a) Reimer, L. *Transmission Electron Microscopy: Physics of Image Formation and Microanalysis*; Springer-Verlag: Berlin, 1984; pp 112−125. (b) Murr, L. E. *Electron and Ion Microscopy and Microanalysis: Principles and Applications*; Marcel Dekker: New York, 1991; pp 590−593. (c) Joy, D. C.; Maher, D. M.; Cullis, A. *J. Microsc.* **1976**, *108*, 185.

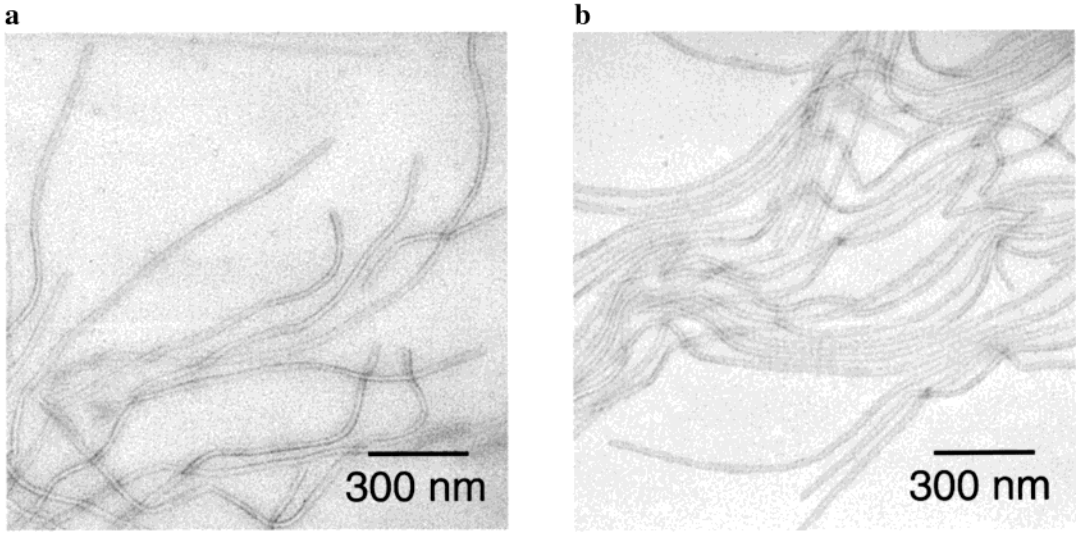

Figure 9. TEM micrographs of PFS_{80}-*b*-$PDMS_{960}$ assemblies prepared in *n*-hexane at 61 °C. In (a) the sample was prepared at 61 °C. In (b) the solution was cooled to room temperature and allowed to age for 2 weeks. Samples for TEM analysis were aerosol-sprayed onto a carbon film.

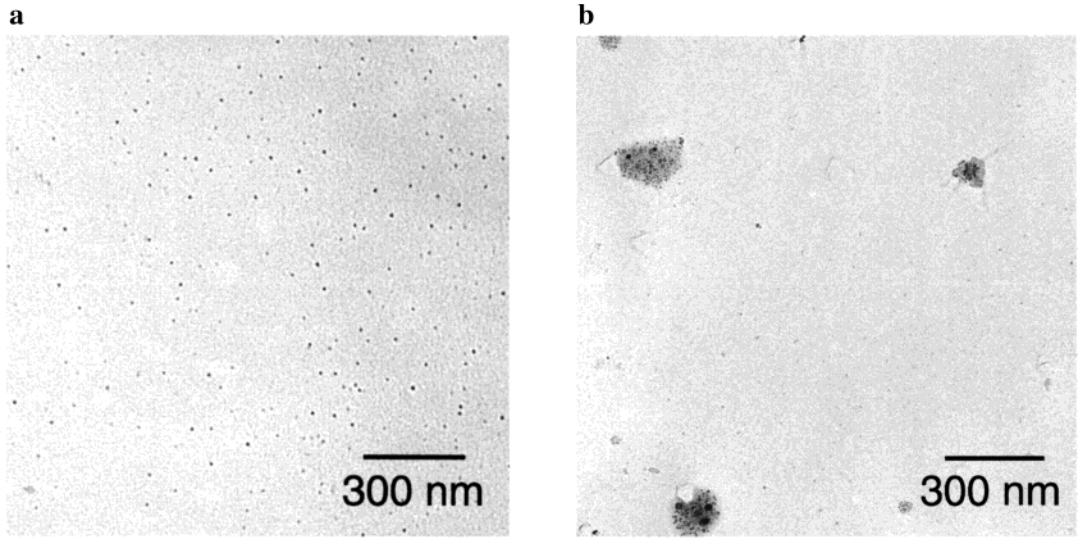

Figure 10. TEM micrographs of PFS_{80}-*b*-$PDMS_{960}$ assemblies formed in *n*-decane prepared at 151 °C. In (a) the sample was aerosol-sprayed at 151 °C onto a carbon film. In (b) the solution was cooled to room temperature over a period of 6h, and a 7-μL drop of the solution was placed onto a precoated copper grid.

in order to image it under TEM. Second, we knew that not all of the small molecules would be encapsulated. We wanted the excess nonencapsulated compound to be volatile enough to evaporate under the high vacuum of the TEM. Third, we wanted the heavy atom in the molecules to be different from iron so that its presence could be detected by EDX. Figure 7a shows a TEM image of the nanotubes with Pb(*n*-Bu)$_4$ inside the cavity. The structures seem dense, but we do not see a dark line due to a cavity densely packed with Pb(*n*-Bu)$_4$. The EDX spectrum shown in Figure 7b confirms the presence of Pb inside the micelles. Although the peak due to Pb is weak, it is comparable in intensity to the Fe peak, which comes from the repeat unit of the crystalline PFS block.

To rule out the possibility that Pb(*n*-Bu)$_4$ is adsorbed on the micelle surface, a control experiment was performed by stirring dense cylindrical micelles (composed of PFS_{50}-*b*-$PDMS_{265}$, 1:5.3 block mole ratio) with Pb(*n*-Bu)$_4$. As in the case of the aggregates formed by PFS_{40}-*b*-$PDMS_{480}$, Pb(*n*-Bu)$_4$ was stirred at room temperature with the micelles of PFS_{50}-*b*-$PDMS_{265}$ in *n*-hexane for 2 days. A sample for TEM was then prepared by spraying an aliquot of the mixture onto a carbon film. The EDX spectrum showed no trace of a peak for Pb in this sample of dense wormlike micelles (Figure 7c). We conclude that the EDX peak for Pb in the PFS_{40}-*b*-$PDMS_{480}$ sample indicates that Pb(*n*-Bu)$_4$ was encapsulated in the interior of a tubular structure. We propose a model for the cross section of the tubes in Figure 12. This drawing does not consider how the chains in the crystalline core are folded, a topic that we consider in more detail below.

Pt/C shadow-casting experiments were performed on the long tubes prepared from PFS_{40}-*b*-$PDMS_{480}$ in *n*-hexane at 61 °C at an angle of 30° (Figure 2d). From the length of the shadows, we calculate a height of 14−17 nm. The height includes the contribution of the PDMS chains. This compares with an overall width of 36−40 nm. From direct observation of the TEM images, we found a tube width of 23 nm and a width of the PFS shell of 7 nm. The combination of the Pt/C shadowing and the direct transmission images indicate that the tubes are wider than they are high. There are two explanations for this

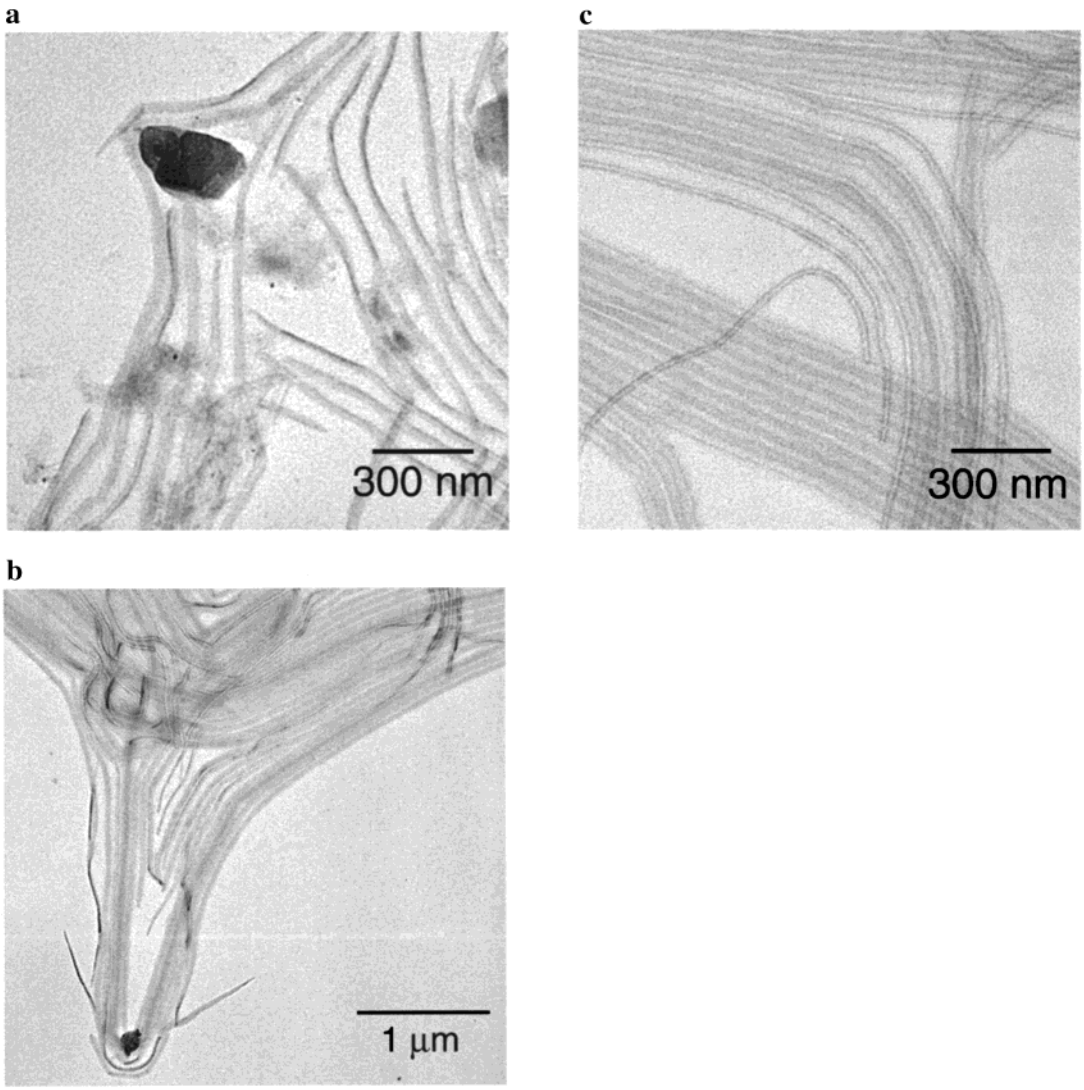

Figure 11. TEM micrographs of PFS_{80}-*b*-$PDMS_{960}$ assemblies formed in *n*-decane at 61 °C. (a) Image of the initially prepared sample. (b) After cooling to 23 °C over 2 h. In (c) the sample was allowed to age for 1 day at room temperature. Samples for TEM analysis were prepared by placing a 7-μL drop of the solution onto a precoated copper grid at room temperature.

Table 2. Persistent Dimensions of Nanotubes Formed under Given Conditions[a]

		n-hexane		*n*-decane	
block copolymer		23 °C	61 °C	61 °C	151 °C
PFS_{40}-*b*-$PDMS_{480}$	d_{cavity}[b] (nm)	9	9	7	7
	PFS wall thickness (nm)	7	7	7	7
	L_{max}[c] (μm)	0.6	4	∼100	∼100
PFS_{80}-*b*-$PDMS_{960}$	d_{cavity}[b] (nm)	11−12	11−12	10−21	−[d]
	PFS wall thickness (nm)	7	7	7	−
	L_{max}[c] (μm)	4	4	∼100	−

[a] These are the "final structures' observed by TEM in our experiments. In each instance, these structures persisted for at least 1 month after the final measurements reported in the text. [b] Cavity diameter [c] Typical contour length of the nanotubes as estimated from the TEM images. [d] No tubular structures formed from this sample.

result. First, the tubular micelles themselves may have an oval shape. Alternatively, the tubes may have a round cross-section in solution but tend to flatten on the substrate. There is no evidence to support either possibility. One can imagine, however, that ribbonlike structures deposited by aerosol spraying might twist prior to deposition. We have never seen any indication of twisted structures in our TEM images.

Solvent Effects on the Persistent Structures. The block copolymers described in this paper have a strong tendency to form nanotubular structures. While we believe that nanotubes represent the equilibrium morphology of the 1:12 block copolymers in *n*-hexane and in *n*-decane at 23 and 61 °C, it is difficult to establish unambiguously that these structures have reached their equilibrium state. For example, it is possible that the structures formed by the lower molecular weight block copolymer have reached their equilibrium diameter, but they may not have reached their equilibrium length. In this section, we are concerned with the structures formed after long aging, and to avoid confusion, we will refer to these as "persistent" structures. In this way, we admit that some aspect of their

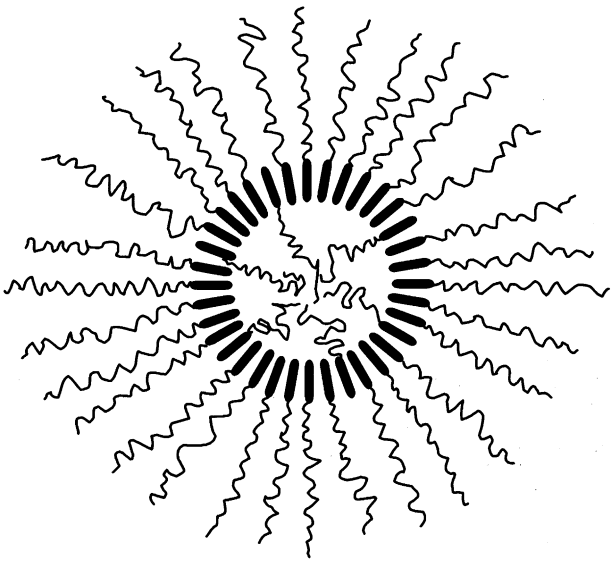

Figure 12. Schematic cross-section of a tube. The PDMS chains are represented by the coils, and the PFS shell is represented by the dark rods.

structure may be kinetically trapped. To provide a framework for our discussion of these structures, we begin with a brief review of the theory of Vilgis and Halperin [11] on the structure of self-assembled structures formed in selective solvents in which the insoluble block is crystalline.

Vilgis and Halperin considered aggregates with a crystalline core, in which the crystalline chain, of length N_B, adopts a tight folding conformation (Figure 13a). A sharp interface divides the crystalline core from the solvent-swollen corona formed by the soluble block of length N_A. The corona chains are treated as though they are grafted to the core at a spacing that depends on the number of folds n_f per core block. The overall shape of the self-assembled structure depends on the interplay between the interfacial energy between the core and the solvent and stretching within the corona. Thus, the response to strong corona chain repulsion is a larger number of thinner folds in the crystalline core-forming chain.

Two interfacial energies enter into the description of the surface free energy per chain ($F_{surface}$), σ_f, the surface tension associated with the fold surface, and σ_l, the lateral surface tension.

$$\frac{F_{surface}}{kT} \approx n_f \frac{\sigma_f a^2}{kT} + n_f^{-1/2} N_B \frac{a^2 \sigma_l}{kT} \quad (1)$$

where a is the size of the monomer, T is temperature, and k is the Boltzmann constant. A representative structure showing the origin of σ_l and σ_f is shown in Figure 13b. The equilibrium free energy is expressed as

$$\frac{F_{surface}}{kT} \approx N_B^{2/3} \frac{\sigma_l^{2/3} \sigma_f^{1/3} a^2}{kT} \quad (2)$$

Within the core, the distance D between grafting sites and the layer thickness l are given by

$$D \approx N_B^{1/3} (\sigma_l/\sigma_f)^{1/3} a \quad (3)$$

$$l \approx N_B^{1/3} (\sigma_f/\sigma_l)^{2/3} a \quad (4)$$

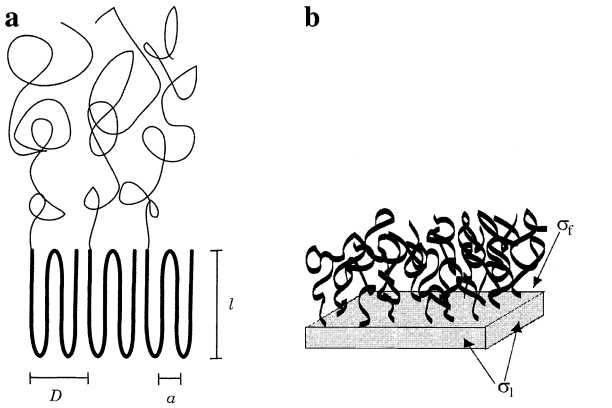

Figure 13. (a) A monolayer layer structure satisfying the Vilgis and Halperin model of how the crystalline block and the soluble block pack in an aggregate formed in a selective solvent. (b) A schematic platelet formed by coil−crystalline block copolymers showing the origin of σ_l and σ_f.

Table 3. Contact Angles Measured for *n*-alkanes on a PFS Film

	θ_{av} (deg)	
solvent	immediately	after 3 min
n-dodecane	26.2	19.0
n-decane	22.7	12.7
n-nonane	17.3	9.8
n-octane	14.3	*a*
n-heptane	10.2	*a*

[a] Solvent evaporated and no measurement was possible.

According to this theory, D/l is proportional to σ_l/σ_f. Thus, one can have an anisotropic structure with many folds per chain (with $D \gg l$) when the lateral surface tension σ_l is much larger than the surface tension σ_f associated with the folds.

In Table 2, we summarize our observations about the long-lived structures formed in hexane and in decane at the temperatures we examined. These are the structures that persist for more than 1 month after structure evolution appears to cease. In the case of PFS_{40}-*b*-$PDMS_{480}$, the cavity diameter of the tubes formed in *n*-decane (7 nm) is smaller than that (9 nm) of the tubes formed in *n*-hexane. We obtained the same result independent of the initial sample preparation temperature. In contrast, the wall thickness inferred from the TEM images is 7 nm in both solvents. In the case of PFS_{80}-*b*-$PDMS_{960}$, the differences in tube width are less clear. The PFS wall thickness remains at 7 nm, despite the doubling of the length of the PFS block. The cavity diameter is larger, but in *n*-decane there is a broad variability in cavity diameter for structures formed at 61 °C, and the system prepared at 151 °C in *n*-decane does not evolve to tubes under the sample aging conditions we employ. The most striking difference between the tubes formed in *n*-hexane and those formed in *n*-decane is the length of the tubes that are formed. The tubular structures formed in *n*-hexane have lengths of at most a few micrometers, whereas the structures formed in *n*-decane have lengths of 100 μm or longer.

To assess whether some feature of the interfacial energy between the core and the solvent is responsible for this change, we measured the contact angle of a series of *n*-alkane solvents on the surface of the PFS homopolymer. The central column of Table 3 lists the values of the contact angle immediately after application of a solvent droplet to the film. This can be thought of as an advancing contact angle. The right-hand column reports the contact angle taken 3 min after the droplet was

applied. Since these droplets contracted in size due to solvent evaporation, they can be thought of as receding contact angles. *n*-Hexane, unfortunately, evaporated too quickly for a contact angle to be measured. Nevertheless, the trend in these values is clear. The interfacial energy between PFS and the lower linear alkanes is much smaller than that between PFS and decane or dodecane. While we cannot separate these surface free energies into their σ_f and σ_l components, we can conclude that $F_{surface}$ (eq 2) is significantly larger for the core in *n*-decane than in *n*-hexane. The massive change in the length of the tubes that form in the two solvents may point to a strongly unfavorable surface energy in *n*-decane associated with the ends of the tubes. The change in solvent may have a much larger effect on σ_l than on σ_f.

There is evidence in the literature based on Flory−Huggins interaction parameters that *n*-decane is a poorer solvent than *n*-hexane for PDMS.[21] Thus, we expect an expanded corona and greater stretching of the corona chains in *n*-hexane than in *n*-decane. From this perspective, we expect a larger value of F_{corona} for the polymer in *n*-hexane than in *n*-decane. The interplay between F_{corona} and $F_{surface}$ allows us to rationalize the larger tube cavity found for structures formed in *n*-hexane. PDMS chains pointing into the tube interior are swollen with solvent and, because of the negative curvature of the interior surface, experience much stronger repulsion than PDMS chains on the exterior surface. Interactions across the tube interior may even limit the extent of stretching accessible to the corona in the tube interior. The system appears to respond by enlarging the cavity rather than by increasing n_f, which would lead to thinner walls.

On the basis of eq 4, one would expect the wall thickness to increase as the molecular weight increases obeying a power law of $^1/_3$. However, this is not the case in our system. As one can observe from Table 2, the wall thicknesses of tubes formed by PFS_{40}-*b*-$PDMS_{480}$ and PFS_{80}-*b*-$PDMS_{960}$ remain constant at 7 nm. Assuming that the PFS blocks undergo chain folding, there would be an average of four folds for PFS_{40}-*b*-$PDMS_{480}$ and eight folds for PFS_{80}-*b*-$PDMS_{960}$ to maintain this shell thickness. Clearly, in the tubes formed by the higher molecular weight block copolymer, the n_f increases in order to minimize the corona repulsion. A possible explanation for the discrepancy between our data and the relation described in eq 4 is that the model does not take into account the F_{corona} of a wormlike, or tubular, micelle that has a curved interface.

Morphology Evolution. One of the most challenging aspects of the research reported here is to understand the factors that affect the changes in morphology that we observe. For example, it is relatively straightforward to rationalize the finding of small spherical micelles in the solution in *n*-decane above the melting temperature of the PFS block. Polymers in which the soluble block is 12 times longer than the insoluble block should form starlike micelles. It is a much bigger challenge to understand how the morphology evolves when this solution of star micelles is cooled and the core attempts to crystallize. The length of the insoluble block has an important influence on the evolution rate. The shorter polymer, PFS_{40}-*b*-$PDMS_{480}$, readily rearranges to form nanotubes, whereas under the conditions reported here, the longer polymer does not. It becomes trapped in some intermediate state.

In the course of this research, we have seen examples in which the initially prepared solution appeared to contain hollow spherical structures (vesicles) in addition to relatively short (60−600 nm) tubular structures and a very small number of longer tubes. One example is shown in Figure 2 for aggregates prepared in hexane at 61 °C. Over time, the sphere population decreases and the tubes grow longer. We infer that the tubes grow at the expense of the spheres perhaps by fusion or coalescence. Evidence for this type of growth mechanism has been reported by Yu and Eisenberg, when they formed "crew-cut" tubules from PS-*b*-PEO.[3e] In that study, the authors described the formation of vesicles in water/DMF mixtures. They reported that, upon aging, their sample evolved. The ratio of tubes to vesicles increased, suggesting that the vesicles were the precursors of the tubules. The authors were able to capture TEM images of possible intermediates of the vesicle-to-tubule transitions. Although there is no theory describing the formation of tubular structures by block copolymers in selective solvents, de Gennes predicted the formation of tubules from lipid-based bilayer membrane vesicles.[22]

One of the most challenging observations to understand is that freshly prepared solutions of PFS_{40}-*b*-$PDMS_{480}$ in *n*-decane at 61 °C show the presence of short dense cylinders and small spheres (Figure 6a). Upon cooling the solution to room temperature, the structures rearrange and grow into well-defined nanotubes. This rearrangement is relatively rapid, occurring in only 2 h (Figure 6b). The nanotubes seen in Figure 6b are significantly wider (21 nm) than the dense cylinders (10−15 nm) formed initially (Figure 6a). We cannot explain why the system initially forms dense cylinders, but we can try to rationalize why these cylinders rearrange to hollow tubes as the solution is cooled.

The χ-parameter for PDMS in *n*-alkane solvents is reported to decrease with increasing temperature.[23] At higher temperatures, the PDMS corona chains are more swollen. Steric repulsion among corona chains promotes curvature at the core−corona interface to increase the volume accessible to each corona chain. When the temperature is lowered, the PDMS chains contract, and this steric repulsion is diminished. Thus, cooling a sample would favor a decrease in the curvature of the interface. Under normal circumstances, this deswelling would provide a driving force for the diameter of core to increase. We speculate that the dense core of the cylindrical structure may not be able to accommodate a decrease in curvature, which would require a rearrangement of the insoluble crystalline PFS block to fill the volume of the core. A rearrangement to a hollow structure with PDMS chains protruding from both the interior and exterior surfaces might allow an optimum balance between n_f and the curvature of the interface.

Our observations have some features in common with results reported by Yu and Eisenberg[3e] for polystyrene-*b*-poly(ethylene oxide) (PS-*b*-PEO) vesicles and tubules in water/DMF mixtures. They found that adding salt to these solutions led to an increase in the diameter of the self-assembled structures. They argued

(21) (a) Hammers, W. E.; De Ligny, C. L. *J. Polym. Sci. Polym. Phys. Ed.* **1974**, *12*, 2065. (b) Chahal, R. S.; Kao, W.-P.; Patterson, D. *J. Chem. Soc., Fraday Trans. 1* **1973**, *69*, 1834.

(22) De Gennes, P.-G. *C. R. Acad. Sci. Ser. 2* **1987**, *304*, 259.

(23) (a) Summers, W. R.; Tewari, Y. B.; Scheiber, H. P. *Macromolecules* **1972**, *5*, 12. (b) Sugayima, K.; Kuwahara, N.; Kaneko, M. *Macromolecules* **1974**, *7*, 66.

that the increase in ionic strength promoted the dehydration (i.e., reduction in swelling) of the corona chains.

Summary

We have examined the self-assembly in hexane and in decane of two PFS-*b*-PDMS block copolymers, each with a block ratio of 1:12. The PFS domains in these structures are crystalline and exhibit WAXS peaks similar to those of PFS homopolymers. Depending on the temperature and the details of sample preparation conditions, we observe by TEM a variety of structures in the initially prepared sample. The final morphology of both polymers in both solvents is that of nanotubes. We were able to confirm the presence of a cavity inside these tubes by encapsulating Pb(*n*-Bu)$_4$. The tubes formed are much longer in decane ($\sim$100 μm) than in hexane (up to 4 μm). In both solvents, the tubes have wall thicknesses, as inferred from the TEM images, of 7 nm for the lower molecular weight block copolymer (PFS_{40}-*b*-$PDMS_{480}$). The interior cavity is wider (9 nm) for the tubes in *n*-hexane than for the tubes in *n*-decane (7 nm). We rationalize these differences by showing that the interfacial energy of the PFS core is significantly higher in *n*-decane than in *n*-hexane.

In conclusion, in this paper we demonstrate that the crystallization of the insoluble block allows access to remarkable tubular assemblies. The hollow structures revealed here are intriguing for encapsulation purposes and because of their redox activity and preceramic potential. Further work aimed at exploring these novel possibilities is in progress.

Acknowledgment. The authors thank NSERC Canada for its support of this research. We thank Dr. Matthew Moffitt for helpful discussions, Mr. Fred Pearson for his technical assistance with the EDX measurements, and Dr. Srebri Petrov for obtaining the WAXS measurements.

JA020349H